HIGHLIGHTS FROM ZEUS

M. WING [*]

Department of Physics and Astronomy
University College London
Gower Street
London WC1E 6BT
UK
E-mail: mw@hep.ucl.ac.uk

Highlights from the ZEUS experiment at HERA as of the DIS06 conference in April
are shown. New results focus on measurements from the HERA II running period
of inclusive DIS at high momentum transfer using polarised leptons and on their
impact in combined QCD and electroweak fits. Investigation of the hadronic final
state, both for inclusive and diffractive reactions, continues to challenge theory.
These are discussed as well as some previously unmeasured hadronic final states.

1. Introduction

As of April 2006, the HERA II running period had surpassed that of the
HERA I phase of operation: $200\,\mathrm{pb}^{-1}$ of data were used for measurements
in this conference; 50% more than in HERA I. The ZEUS collaboration has
also published its first paper using the HERA II data on "Measurement
of high-Q^2 deep inelastic scattering cross sections with a longitudinally
polarised positron beam at HERA" [1]. The results of this paper along with
the higher-statistics measurement using incoming electrons are the focus
of this contribution. However, the data from HERA I, where the detector
is well understood continues to provide a wealth of information on the
hadronic final state, perturbative QCD and diffraction.

2. High Q^2 physics

The first HERA II publication from ZEUS is both a measurement of a
new process and an important step towards further results. Cross sections

---

[*]On behalf of the ZEUS Collaboration

2

were measured in charge (CC) and neutral current (NC) DIS and are well described by Standard Model predictions. Although the expected strong dependence of the CC cross section on the polarisation of the incoming positron was observed, the far weaker dependence of the NC cross section was not observed at a significant level. Using a sample about a factor of four larger in luminosity, this effect has been observed in the recently taken polarised electron data [2], shown in Fig. 1.
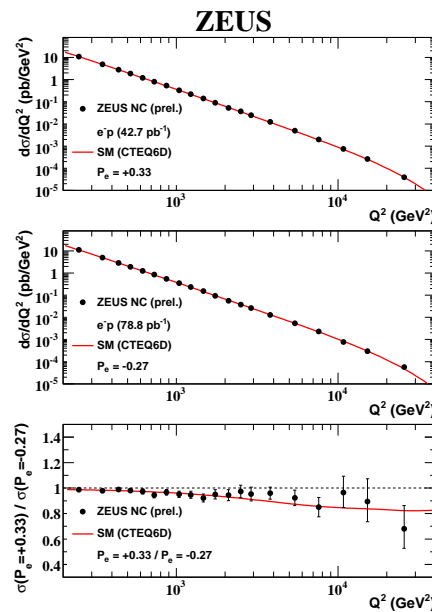

Figure 1.   The NC DIS cross section versus Q^2 for positive (top) and negative (middle) electron polarisations and the ratio of the two polarisations (bottom). The data are compared to the Standard Model prediction.

The total CC cross section for the electron and positron data at positive and negative polarisations [3] is shown in Fig. 2 compared with the unpolarised measurements from HERA I. The data are well described by predictions of the Standard Model. Fitting the data and extrapolating to polarisations, $P_e = \pm 1$, yields values consistent with zero and hence consistent with absence of right-handed charge currents in the Standard Model.

Single and double differential cross sections have also been measured for both NC and CC processes. Using an electron data sample about eight times larger than previously, an improved extraction of the parity-violating
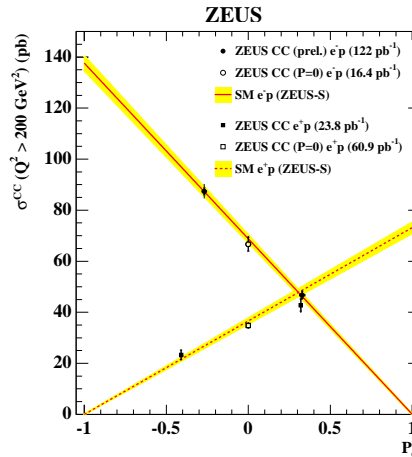
Figure 2. Total CC DIS cross sections versus the polarisation for electrons and positrons. The data are compared to the Standard Model prediction.

structure function, F_3, has been made from the NC cross sections [2]. However, the statistical errors on this measurement still dominate and so will be continually improved until the end of HERA running.

All these data have been used in a combined electroweak and QCD fit [5], based on the previous ZEUS-JETS fit [4] to the parton densities. The new parton densities are consistent with those obtained previously which is a good cross check of both the new data and fit procedure. Small improvements in the precision of the determinations are observed for the d-valence, sea and gluon distributions. However, a significant improvement is seen for the u-valence as expected from including high-precision electron data. The QCD fit will be further improved with new jet measurements [6] as well as the inclusion of other processes sensitive to the structure of the proton such as heavy quark and prompt photon production. A complete description of many different processes will provide a compelling test of QCD and precise measurements of the strong coupling and the parton density functions.

Some of the electroweak parameters, the axial and vector couplings of the u and d quarks, extracted in the combined fit are shown in Fig. 3. The improved precision of the vector couplings due to the inclusion of polarised electron data from HERA II can be seen when comparing the ZEUS result to that from H1 which only used the HERA I data sample. The ZEUS measurements are also competitive, particularly for the u quark, with those from LEP and significantly better than the CDF determinations.
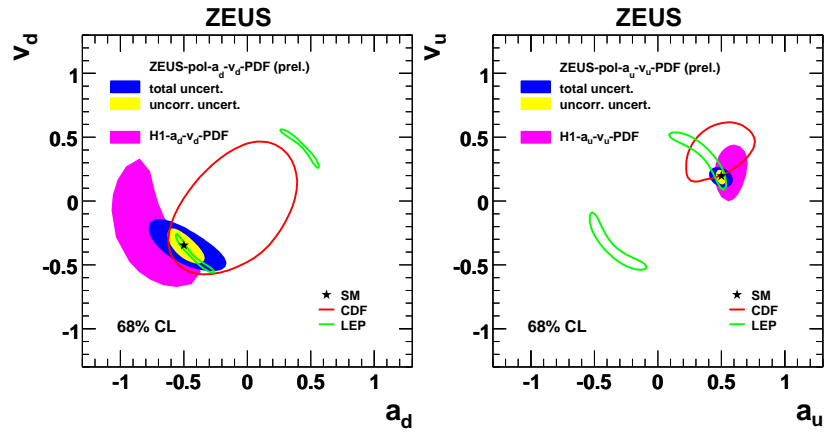
4

Figure 3.   Axial and vector couplings of the u and d quarks extracted from a combined electroweak and QCD fit. The ZEUS measurements are compared to those from other experiments.

As well as verifying the Standard Model over a large energy range, another aspect of measuring processes at the highest possible scale is to look for physics beyond the Standard Model. The ZEUS collaboration continues to search for events such as isolated leptons at high transverse momentum with a large missing transverse momentum where H1 has observed differences with the Standard Model prediction [7]. ZEUS has adapted their analysis strategy to more closely follow that of H1 and has now analysed all data between 1998-2005 with an electron in the final state. In ZEUS, the rate of produced events is independent of the incoming lepton beam and is consistent with the Standard Model as can be seen in Table 1. This is somewhat in contrast to the results from H1 although statistical fluctuations cannot be ruled out.

Table 1.   Number of events found by H1 and ZEUS which contain isolated high p_T leptons compared with the Standard Model and the fraction of those which are W events.

Isolated e candidates	$P_T^X > 25$ GeV
ZEUS (prel.) 98-05 e^-p (143 pb^{-1})	3/2.9±0.5(53%)
ZEUS (prel.) 99-04 e^+p (106 pb^{-1})	1/1.5±0.1(78%)
ZEUS (prel.) 98-05 $e^{\pm}p$ (249 pb^{-1})	4/4.4±0.5(61%)
H1 (prel.) 94-05 $e^{\pm}p$ (279 pb^{-1})	11/4.7 ± 0.9 (69%)

3. Diffraction

Many recent measurements of the diffractive structure function [10] have allowed extractions of the diffractive parton density functions (DPDFs) to be made. As in inclusive production, the factorisation theorem entails that DPDFs extracted from one process can be used to predict the rate in another. This is under intensive study at HERA with measurements made of jet and charm rates in both photoproduction and DIS. In Fig. 4, such a measurement is shown for dijet production in diffractive DIS compared with different DPDFs [9]. There is a large spread in the predictions, resulting from differences in the data to used make extractions of the DPDFs. This demonstrates that these dijet data are sensitive to the DPDFs and could be used in global fits to constrain their form. It also shows that more understanding of the inclusive diffractive data is needed before stronger statements can be made about confirmation or breaking of factorisation.
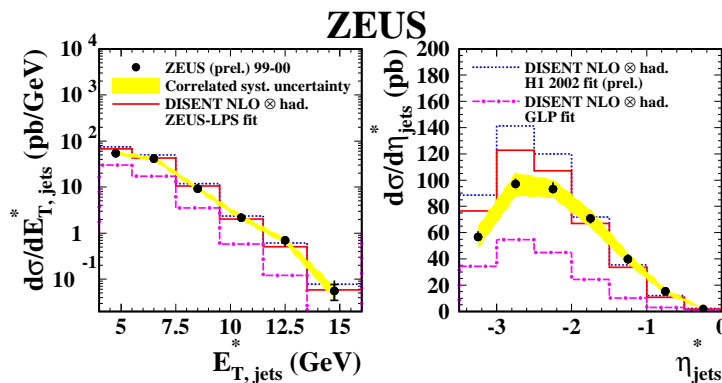

Figure 4.   Cross sections for dijet production in diffractive DIS. The data are compared to a next-to-leading-order (NLO) QCD calculation incorporating different diffractive parton density functions.

Similar ideas can be probed in events with a leading neutron in the final state. If this process is mediated by one-pion exchange, then PDFs can also be extracted and used to predict rate for other processes. In the following [11], the production of leading neutrons has been measured and compared, amongst other things, to models of one-pion exchange. The p_T^2 distribution of the neutron has been measured and the slope of the distribution parametrised as $e^{-bp_T^2}$. The value of b is plotted against the fraction of the beam's energy carried by the neutron, x_L, in Fig. 5. None of

6

the models shown (many more exist which give a poorer description of the data) gives a good description of the data although the general features of a rise to high x_L and a turn-over are observed. These data have excellent discriminating power for these and future models.
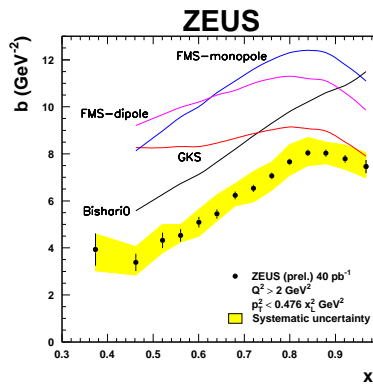

Figure 5.   Measurement of the b slope in leading neutron production compared with various models.

4. The hadronic final state

Data from the HERA I running period is still producing first-time and high-precision measurements, aided by a mature understanding of the detector.

The production light nuclei in elementary interactions is unclear and has increased interest recently due to the relation with pentaquark searches. Therefore a new measurement is presented of the observation of anti-deuteron production in DIS. The anti-deuteron candidate is produced at the primary interaction point and is identified using the energy loss measured in the central tracking detector. In Fig. 6, the ratio of anti-deuteron and anti-proton rates are shown compared with a measurement in photoproduction from H1; the rates are the same in the two kinematic regions. Comparison of these data with e.g. the coalescence model has the potential to reveal a lot about light nuclei production; measurement of deuteron production should reveal more.

Jet production in photoproduction continues to challenge QCD calculations and models. A recent measurement of multijet states in photoproduction [13] intrinsically probes high-order QCD and is also sensitive to models
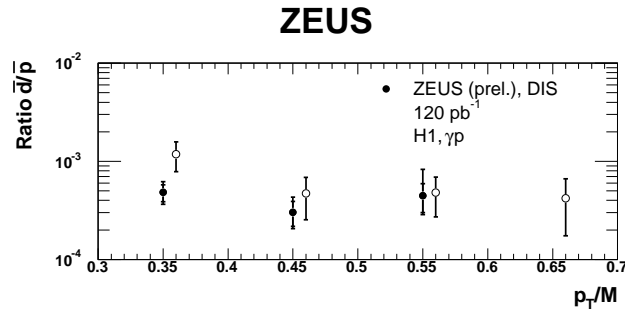
ZEUS

Figure 6.   Comparison of anti-deuteron to anti-proton production rates in deep inelastic scattering and photoproduction.

of the underlying event, such as hard multi-parton interactions. Cross sections for three- and four-jet production are shown versus $x_\gamma^{\rm obs}$, the fraction of the photon's momentum participating in the multijet system, in Fig. 7. The cross section at low $x_\gamma^{\rm obs}$, where the photon is hadron-like, is significant and is better described by theories incorporating an underlying event model. The data have also been compared to a tree-level calculation - disagreements are observed - and would benefit enormously from a full NLO QCD calculation.
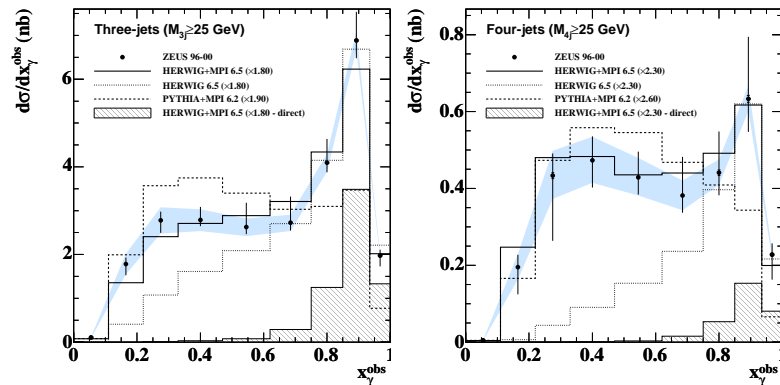

Figure 7.   Cross section versus $x_\gamma^{\rm obs}$ for three- (left) and four-jet (right) photoproduction compared with predictions from Monte Carlo models.

Another area where current theoretical calculations are limited are dijet correlations in charm photoproduction [14]. The inclusive-jet cross section

8

in charm photoproduction is adequately described by NLO QCD. However, as can be seen in Fig. 8, the difference in azimuthal angle of two jets is poorly described for the region $x_\gamma^{\mathrm{obs}} < 0.75$. The HERWIG Monte Carlo model which incorporates leading-order matrix elements followed by parton showers and hadronisation describes the shape of the data well. This indicates that for the precise description of charm dijet photoproduction, higher-order calculations or the implementation of additional parton showers in current NLO calculations are needed.
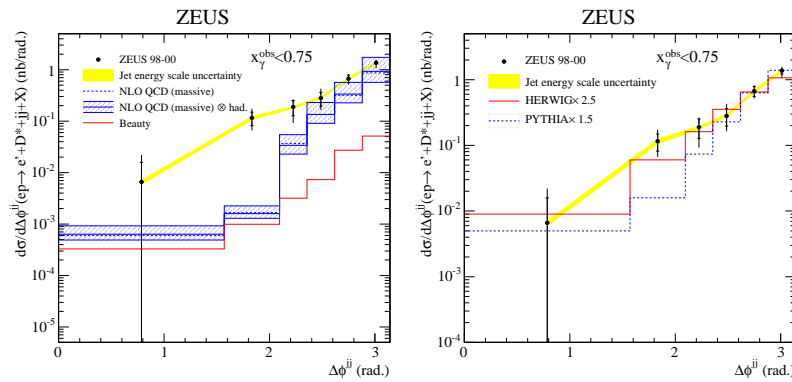

Figure 8.   Charm dijet photoproduction cross sections compared to NLO QCD (left) and Monte Carlo models (right).

References

1. ZEUS Coll., S. Chekanov et al., Phys. Lett. **B 637** (2006) 210.
2. S.U. Noor, these proceedings.
3. H. Kaji, these proceedings.
4. ZEUS Coll., S. Chekanov et al., Eur. Phys. J. **C 42** (2005) 1.
5. S. Shimizu, these proceedings.
6. T. Schoerner-Sadenius, these proceedings; M. Jimenez, these proceedings.
7. E. Perez, these proceedings.
8. M. Corradi, these proceedings.
9. A. Bonato, these proceedings.
10. P. Newman, these proceedings; H1 Coll., A. Aktas et al., DESY-06-048, Submitted to Eur. Phys. J.; H1 Coll., A. Aktas et al., DESY-06-049, Submitted to Eur. Phys. J.; ZEUS Coll., S. Chekanov et al., Nucl. Phys. **B 713** (2005) 3; ZEUS Coll., S. Chekanov et al., Eur. Phys. J. **C 38** (2004) 43;
11. M. Soares, these proceedings.
12. T. Matsumoto, these proceedings.
13. T. Namsoo, these proceedings.
14. ZEUS Coll., S. Chekanov et al., Nucl. Phys. **B 729** (2005) 492.